Functional Materials 17, No.1 (2010)

Synthesis of Y_2O_3 and Y_2O_3:Nd^{3+} monodisperse crystalline nanospheres by homogenous precipitation

Yu.I.Pazura, V.N.Baumer, T.G.Deyneka, O.M.Vovk, R.P.Yavetskiy

Institute for Single Crystals, STC "Institute for Single Crystals", National Academy of Sciences of Ukraine, 60 Lenin Ave., 61001 Kharkiv, Ukraine

Received October 30, 2009

Y_2O_3, Y_2O_3:Nd^{3+} (1–10 at. %) monodisperse crystalline spheres in interval 100-260 nm diameter with dispersion of size ≤10 % have been synthesized from aqueous solution by homogenous chemical precipitation. The formation process of cubic yttrium oxide nanospheres during thermal decomposition of amorphous precursor has been studied. The precipitation parameters (concentration of yttrium, neodymium ions, as well as urea concentration) have been found to influence considerably the size, shape, dispersion, and agglomeration degree of resultant powders.

Методом гомогенного химического осаждения из водных растворов получены монодисперсные кристаллические сферы Y_2O_3, Y_2O_3:Nd^{3+} (1–10 ат. %) с диаметром в интервале 100-260 нм с дисперсией по размеру ≤10 %. Изучен процесс формирования наносфер кубического оксида иттрия при термическом разложении аморфного прекурсора. Установлено влияние параметров процесса осаждения (концентраций исходных реагентов — ионов иттрия, неодима, а также карбамида) на размер, дисперсию и степень агломерации порошков.

1. Introduction

The monodisperse spherical luminescent particles of rare earth oxides are under intense studies for optoelectronics, biomedical applications, for laser and scintillation techniques. Such particles are of good promise for use as initial "building block" for the following consolidation in high-density luminescent materials 2D or 3D [1,2]. The particular interest for the spherical monodisperse nanoparticles is connected with possibility of their utilization for fabrication of transparent ceramic [3]. In the current optical ceramic production technology, the compaction stage is considered as the most critical one [4]. The packing defects in the green body cause decreased ceramics density, residual porosity and thus degradation of its optical properties. Therefore, the initial nanopowders for optical ceramics should meet the following requirements: the spherical form of the particles, the particle size of about 100 nm and the narrow particle size distribution range [5]. Obviously, the compaction of the monodisperse nanospheres allows provides a more homogeneous packing of the particles in the compact and the higher initial density as compared to nanopowders with undefined morphology. This promotes an efficient and homogeneous densification of ceramics at the sintering stage. For example, the molding of monoclinic Y_2O_3 spheres with particle size within 2–40 nm range (average diameter of 10–15 nm) by magnet-pulsed compaction permits to attain the compact density of 83 % of the theoretical value [6], that considerably exceeds the 74 % value for the hexagonal closest packing of the spherical particles. Therefore, the preparation of the monodisperse spherical nanoparticles with sizes ranging from 50 to 250 nm is a sig-

nificant task in the advanced powder technology of high-density consolidated optical materials creation.

Nowadays, a number of methods are being applied to produce spherical oxide particles, namely, spray pyrolysis [7], the Pechini sol-gel technology [8], solvothermal [9] and hydrothermal [10, 11] methods, the target laser evaporation [12]. However, none of these methods provide the nanoparticles with the required characteristics. For instance, Y_2O_3 spherical particles can be obtained by laser evaporation of target; however, Y_2O_3 powders are formed in metastable state (monoclinic modification) and require a high-temperature annealing to convert them into cubic structure, thus increasing their agglomeration [13]. The homogenous precipitation from aqueous solution is considered as the most promising method to obtain the crystal nanospheres of rare earth oxides with the narrow particle size distribution [14]. The precise control of precipitation conditions (synthesis temperature, pH value, reagent concentrations, order and speed of their mixing) allows one to adjust the phase and chemical composition of nanopowders, their crystallinity, dispersion and agglomeration degree, and the distribution homogeneity of the activator ions. Moreover, this method is simple enough in terms of technological realization.

The pure and neodymium-doped yttrium oxide is an excellent optical material for IR windows and active medium of the solid-state lasers. Recently, Y_2O_3-based optical ceramics was described in literature [13, 15, 16], as well as the preparation techniques of yttrium oxide-based spherical particles (see [1, 17, 18], and references therein), generally, for application as red phosphors. Preparation of the Y_2O_3:Nd^{3+} spherical particles for optical ceramics has not been reported in modern publications. The aim of this work was to synthesize and characterize the monodisperse crystalline Y_2O_3 and Y_2O_3:Nd^{3+} (1–10 at. %) spheres of different diameter by homogenous precipitation from aqueous solution.

2. Experiment

Y_2O_3 and Y_2O_3:Nd^{3+} (1–10 at. %) nanospheres were synthesized from yttrium and neodymium nitrate solutions using homogenous precipitation by urea. The yttrium and neodymium nitrate solutions were prepared from corresponding oxides Y_2O_3 (>99.99 % pure) and Nd_2O_3 (>99.99 % pure) by dissolving them under heating in the proper amount of nitric acid. The concentration of the yttrium solutions was varied in the 0.005–0.5 mol/L range. The urea solutions in concentrations varying from 0.3 to 4.0 mol/L were used as the precipitants. The initial component mixture was homogenized under constant stirring for 2 h and then was heated on a water bath to 90°C. After reacting at 90±1°C for 2 h, the suspension was cooled to ~50°C, and the resultant colloidal particles were separated via suction filtration through a membrane filter. The precipitate was washed four times with distilled water and one time with anhydrous ethanol in order to remove the reaction by-products. Then the precursor obtained was dried in an air at 25°C and was used for further studies.

The differential thermal (DTA) and thermal gravimetric (TG) analyses were carried out using a MOM Q-1500D derivatograph in air atmosphere in the 20–1000°C temperature range with the heating rate of 10°C/min. The phase identification was performed via X-ray diffraction (XRD) on a SIEMENS D-500 X-ray diffractometer using nickel filtered Cu K_α radiation. The phases were identified using PDF-4 card file and EVA retrieval system, included in the diffractometer software. The powder morphology was examined using a transmission electronic microscope TEM-125 operated at 100 kV accelerating voltage. Prior to the microscopic examination, the powder was subjected to ultrasonication using ultrasonic dispergator UZDN-A at frequency of 22 kHz during 45 s. The bidistilled water was used as the working medium. The average particle size and distribution were estimated from TEM micrographs by collecting data for at least 200 particles.

3. Results and discussion

It is known that decomposition of urea during heating of its solution up to >85°C results in slow and homogeneous release of precipitating ligands, mainly OH^- and CO_3^{2-} ions, into the reaction system [19]. These ions react with yttrium ones to form yttrium precursor. The reaction mechanism of the formation of yttria particles through homogeneous precipitation is claimed to include three distinct steps: 1) decomposition of urea, 2) hydrolysis of yttrium ions (Y^{3+}), and 3) precipitation reaction (1). Briefly, the last step of this reaction can be presented as follows:

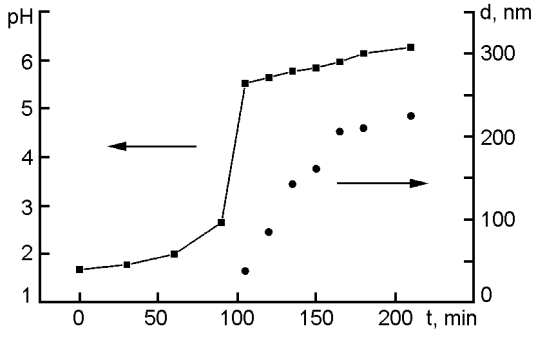

Fig. 1. Variations of the reaction mixture pH and the precursor particle diameter in time ($c(Y^{3+})$ = 0.015 mol/L, c(urea) = 0.5 mol/L, temperature 90°C).

$$[Y(OH)]^{2+} + CO_2 + H_2O \rightarrow \quad (1)$$
$$\rightarrow Y(OH)CO_3 \cdot H_2O + H_2^+.$$

The time dependence of initial solution pH and average diameter of precipitated particles is given in Fig. 1. The precursor particles start to form after reaching of the equivalency point (pH = 4). The growth of the precipitated particles in time is accompanied by pH value increase, and then the hydrogen ion exponent attains saturation. The intensive growth of $Y(OH)CO_3$ precursor spherical particles occurs in the pH range from 5.5 to 6, and finishes at pH = 6.5–7. At these conditions, the particle diameter become the constant value of about 255 nm and further remains unchanged.

The DTA and TG curves of the precursor obtained after drying at 25°C are presented in Fig. 2. According to TG data, the stepwise decomposition of the yttrium oxide precursor is accompanied by a total weight loss of 39 %. Two endothermic peaks in the DTA curve at 170 and 257°C were assigned to the removal of molecular and hydration water, while the broad peak in the 400–600°C temperature range, to formation of non-identified intermediate phases. According to [20], the double endothermic peak in the 600–700°C temperature range could be due to simultaneous decomposition of complex yttrium carbonates (for example, $Y_2O(CO_3)_2$, $Y_2O_2CO_3$), and crystallization of yttrium oxide (i.e. exothermic and endothermic peaks are superposed).

The effect of reactant concentrations on the shape and size of yttrium oxide precursor spherical particles are presented in Fig. 3. In this experiment, the yttrium nitrate concentration was varied in the 0.005–0.5 mol/L range at constant urea

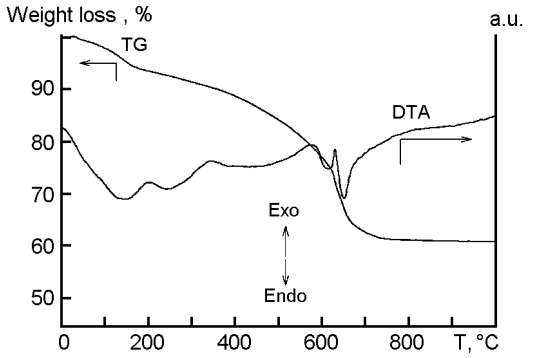

Fig. 2. DTA/TG curves of the precursor produced by homogeneous precipitation with urea.

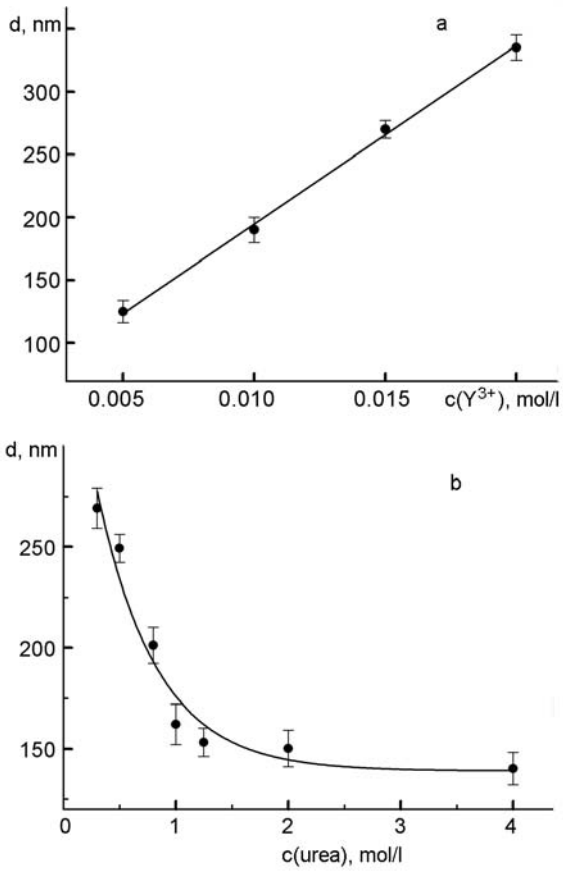

Fig. 3. Average diameter of the precursor particles as a function of the Y^{3+} ions concentration (c(urea) = 0.5 mol/L) (a) and urea concentration ($c(Y^{3+})$ = 0.015 mol/L) (b).

concentration, or urea concentration was varied in the 0.3–4.0 mol/L range at constant yttrium concentration. The initial reactant concentrations influence strongly the average particle diameter. As is seen in Fig. 3a , the average particle diameter varies linearly from 125 nm to 335 nm for yttrium concentration between 0.005 and

0.02 mol/L. Below 0.02 mol/L, the particles do not agglomerate, and the particle size distribution is really monodisperse (the standard deviation does not exceed 7–9 %) . The higher yttrium concentration is, the more polydisperse particles are formed, and at yttrium concentration between 0.02 and 0.03 mol/L, the deviation in particle size distribution increases up to 67 %. Moreover, the particle trend to aggregate, and finally, at concentration above 0.025 mol/L, the agglomerates are formed reaching several micrometers in diameter. One of the reasons causing particle agglomeration is decrease of solution zeta potential as a function of yttrium concentration [19]. The particle diameter dependence on urea concentration is given in Fig. 3b. Changing the urea concentration from 0.3 to 2.0 mol/L causes the average diameter of Y_2O_3 particles to be diminished from 270 to 150 nm. The Y_2O_3 particle size distribution in the mentioned concentration range is almost constant and does not exceed 10 %. Moreover, in the whole concentration range studied, the precipitate maintains spherical shape. Therefore, adjusting the reactants concentrations allows one to control the shape, size, and size distribution of Y_2O_3 nanospheres.

The XRD spectra of the Y_2O_3 nanopowders calcined at different temperatures are shown in Fig. 4. The yttrium oxide precursor and the powders calcined up to 500°C were found to be amorphous. Formation of the cubic Y_2O_3 is already registered at 600°C. The calcination temperature rise results in increasing intensity of the diffraction peaks as well to their narrowing, pointing out the increasing average crystallite size. In fact, the crystallite size of the Y_2O_3 powders determined by the Scherrer formula increases from 20 to 109 nm when temperature rises from 600°C to 1200°C. Simultaneously, the lattice parameter a is diminished from 10.6143(4) to 10.60508(10) Å, and at T = 1200°C approaches the theoretical value for Y_2O_3 a = 10.604 Å, thus indicating the improving crystalline structure perfection of the Y_2O_3.

Because the Y_2O_3 powders are planned to use in optical ceramic fabrication via vacuum sintering, it is very important to study their morphological changes during the calcination. According to DTA and XRD data, the crystalline yttrium oxide is formed from amorphous precipitate above 600°C. The morphology evolution of Y_2O_3 nanospheres with calcination temperature is given in Fig. 5. The calcination temperature is seen to affect considerably the morphology

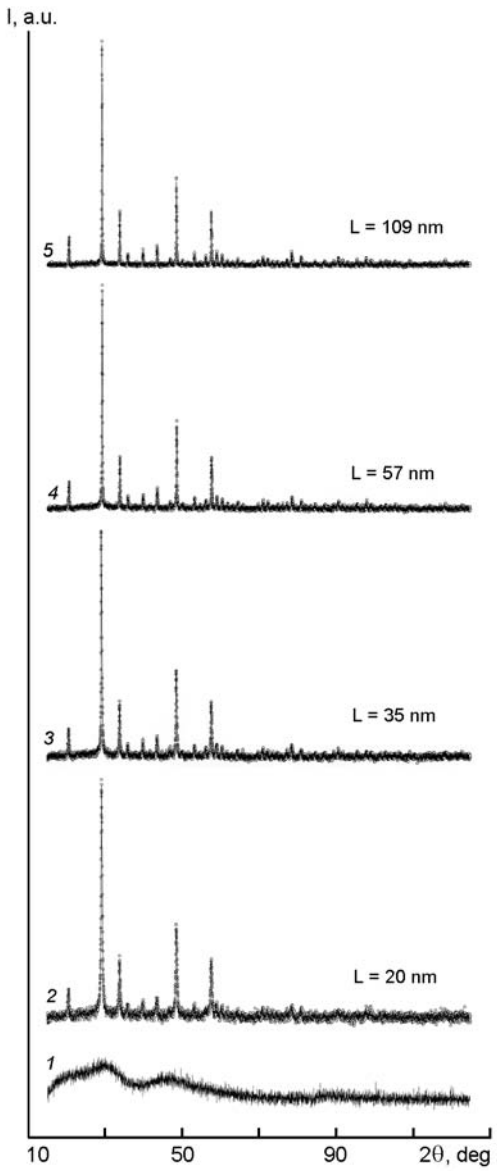

Fig. 4. XRD spectra of the Y_2O_3 powders calcined at 400°C (*1*); 600°C (*2*); 800°C (*3*); 1000°C (*4*) and 1200°C (*5*).

and size of synthesized powders. The diameter of the powders calcined at T = 750°C decreases by 23±1 % due to decomposition of precursor (Fig. 5, b). Moreover, the surface of crystalline spherical particles becomes slightly rough, mainly due to evaporation of structural water and CO_2. Annealing of the powders does not affect the particle size distribution. The crystallite size increase in the 600–1000°C temperature range determined from the XRD data (Fig. 4) occurs without changing of the particle diameter, indicating that the primary recrystallization takes place inside the spherical particles, probably via joining of

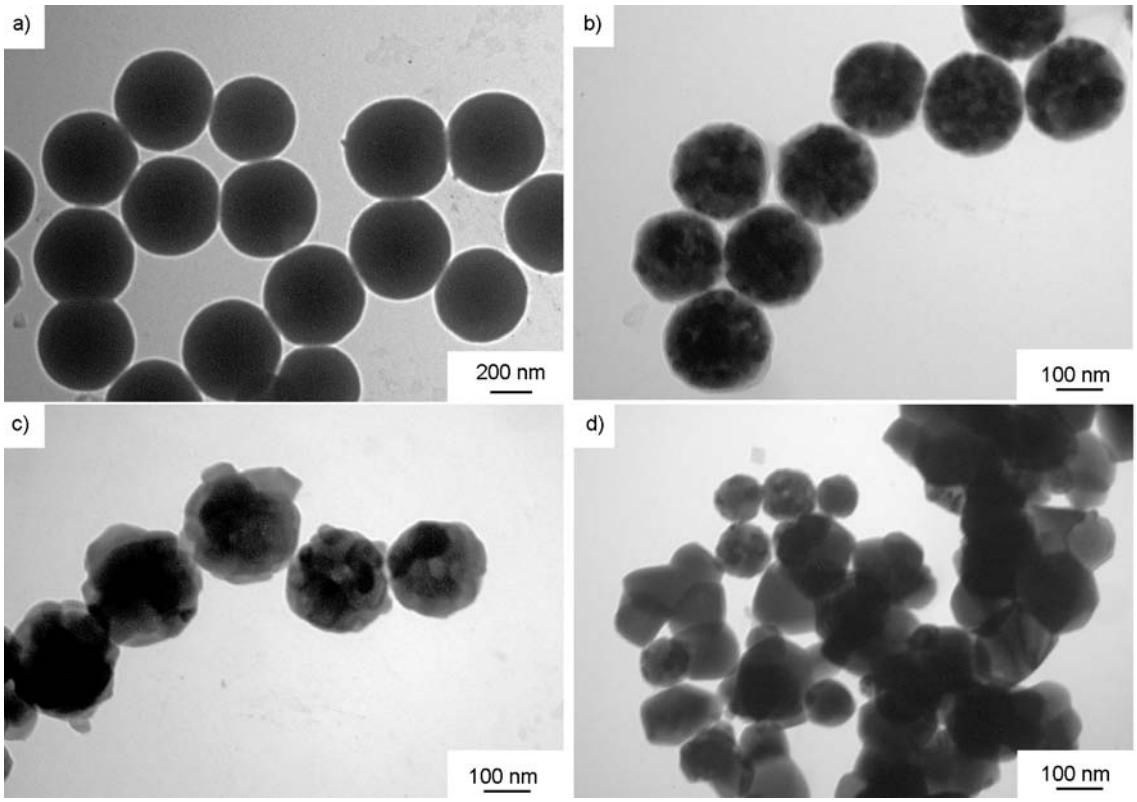

Fig. 5. TEM of precursor (a) and Y_2O_3 nanospheres, calcined at 800°C (b); 1000°C (c) and 1200°C (d).

adjacent crystallites. The roughness of nanospheres increases slightly with calcination temperature increase up to 1000°C, but the particles maintain their individuality. The sintering of the particles with partial lost of their spherical shape starts at the temperature of 1000°C with formation of contact necks between the particles (Fig. 5, c). The further temperature increase results in formation of hard agglomerates due to intensive sintering of the powders (Fig. 5, d). The morphological characteristics of resulting powders became very similar to the ordinary nanopowders, indicating that additional technological stages (mechanical grinding) are required to use them as starting materials for optical ceramics.

The morphology of Y_2O_3 nanosphere of different diameter is shown in Fig. 6. Each spherical particle contains several crystalline blocks of nearly spherical shape and about 30 nm diameter, which is equal to crystallite size determined by XRD (Fig. 4), in other words, the particles are polycrystalline. Fig. 6 d, inset, shows selected area electron diffraction (SAED) pattern from individual spherical Y_2O_3 particle. The SAED pattern contains individual reflections as well as diffraction rings confirming the polycrystalline nature of the sample. The similar structure of Y_2O_3:Eu^{3+} spherical particles obtained by spray pyrolysis have been recently observed in [7]. The average crystallite block size in the particles of different diameters falls within 30–40 nm range. The small size of the crystallites is very favorable for high activity of the powders and their effective densification into high-density pore-free optical ceramic. Furthermore, the initial crystallites form the particles of the equilibrium spherical shape, thus decreasing the powder agglomeration and facilitating their compacting (Fig. 6, a–d). Therefore, we believe that morphological peculiarities of Y_2O_3 spherical particles obtained (polycrystalline structure, monodispersity, spherical shape, low agglomeration degree) are very favorable for their use in optical ceramics fabrication.

The doping of yttrium oxide with neodymium ions (1–10 at. %) results in linear increase of the lattice parameter a according to the Vegard rule, evidencing the formation of the substitutional solid solution $(Y_{1-x}Nd_x)_2O_3$ (Fig. 7a). The extension of the lattice parameter is connected with larger ionic radius of neodymium ions compared to yttrium ones ($r(Nd^{3+})$ = 1.25 Å, $r(Y^{3+})$ = 1.16 Å for coordination number 8). The presence of neodymium ions not only influences the lattice

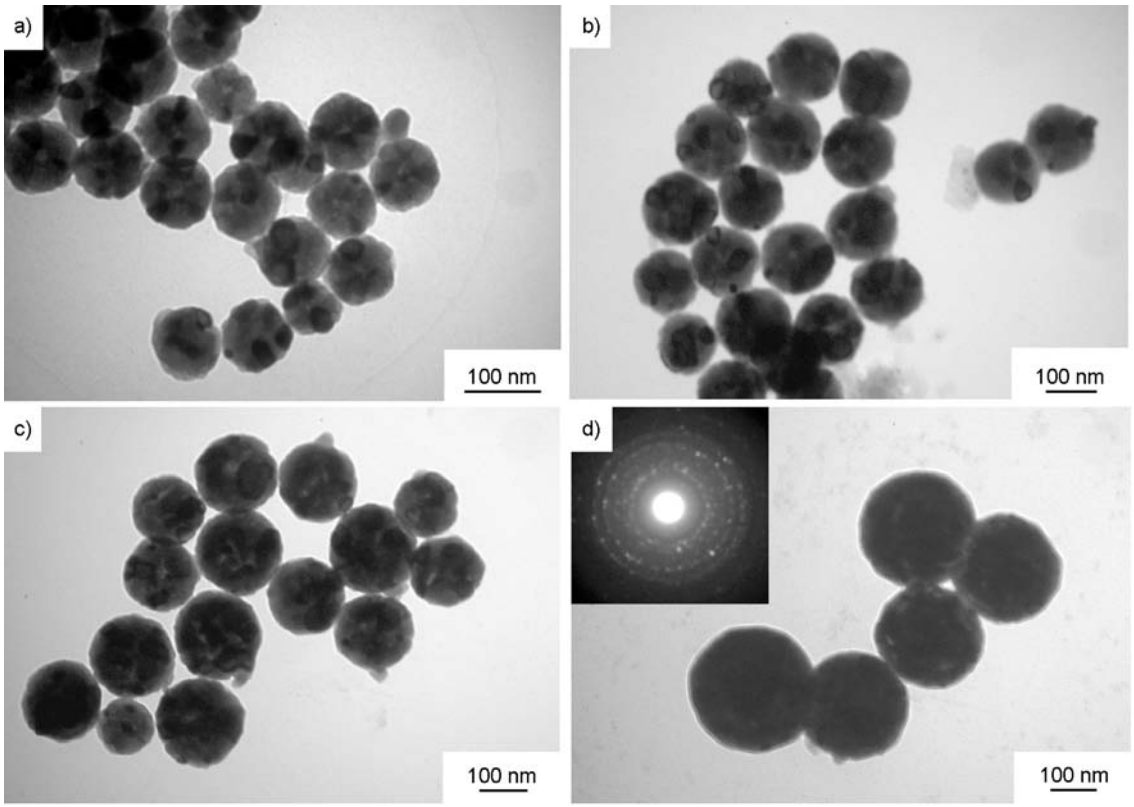

Fig. 6. TEM of Y_2O_3 calcined at 750°C depending on the yttrium ions concentration, mol/L: a) 0.005; b) 0.01; c) 0.015; d) 0.02. ($c((NH_2)_2CO)$ = 0.5 mol/L). Inset in Fig. 6 d shows SAED pattern from an individual spherical Y_2O_3 particle.

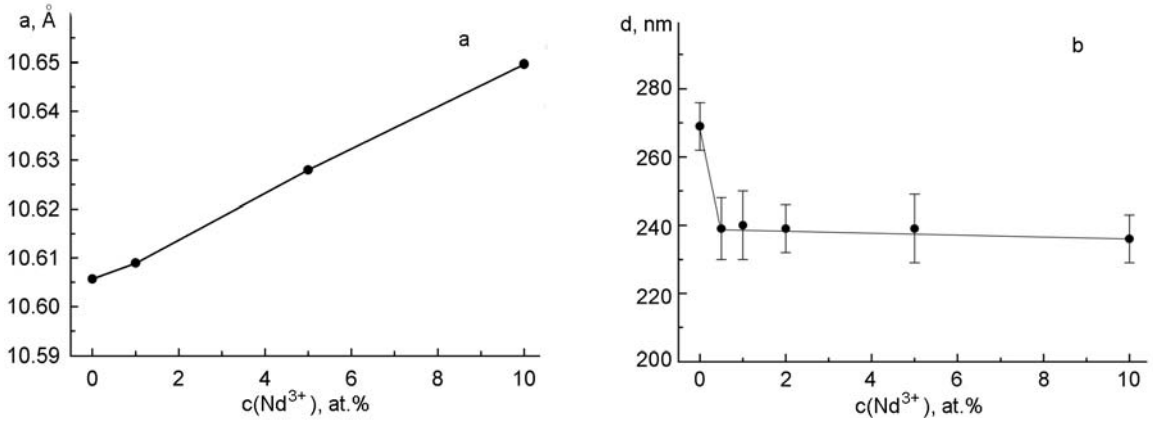

Fig. 7. The lattice parameter a (a) and average particle diameter (b) of Y_2O_3:Nd^{3+} particles as a function of the Nd^{3+} ions concentration ($c((NH_2)_2CO)$ = 0.5 mol/L, $c(Y^{3+})$ = 0.015 mol/L).

constant, but also the nucleation processes in the colloidal systems, the diameter of activated yttrium oxide particles being smaller as compared to undoped ones (Fig. 7b). The similar effect has been observed before for another mixed oxide system Y_2O_3–Gd_2O_3 [14]. As the formation of the colloidal spheres occurs via nucleation/growth process [19], the homogeneous nucleation rate depends on the supersaturation degree, that is, the nucleation starts only when the supersaturation reaches a certain critical value. In accordance with the lanthanide contraction phenomenon, $Y(OH)CO_3$ possesses higher solubility in water as compared to $Nd(OH)CO_3$, and, consequently, has a lower supersaturation value. This means that $Y(OH)CO_3$ nuclei are relatively unstable, therefore, in mixed Y/Nd system we can suppose the predominant formation of

$Nd(OH)CO_3$ nuclei. The precipitation and growth of $Y(OH)CO_3$ will occur via heterogeneous nucleation on the already formed $Nd(OH)CO_3$ particles, exactly as in the Y/Gd system [14]. So, we belive that the Nd^{3+} ions concentration increase provides an increased nucleation density and $Y_2O_3:Nd^{3+}$ spherical particles obtained have smaller diameter.

4. Conclusions

The crystalline Y_2O_3, $Y_2O_3:Nd^{3+}$ monodisperse nanospheres of 100 to 260 nm diameter, narrow particle size distribution (max. 10 %) have been obtained by homogeneous precipitation from aqueous solution. The morphology evolution of Y_2O_3 nanospheres with calcination temperature increase has been studied. It has been determined that the sintering of the particles with partial lost of their spherical shape starts at 1000°C. It has been shown that adjusting the reactant concentration (yttrium ions, neodymium ions and urea) allows one to control the shape, size, and size distribution of Y_2O_3 nanospheres. Finally, we believe that morphological peculiarities of Y_2O_3 spherical particles obtained (polycrystalline structure, monodispersity, spherical shape, low agglomeration degree) are very favorable for their effective densification into high-density optical ceramic.

References

1. S.H.Cho, S.H.Kwon, J.S.Yoo et al., *J. Electrochem. Soc.*, **147**, 3143 (2000).
2. S.-E.Lin, B.-Y.Yu, J.-J.Shuye et al., *J. Am. Ceram. Soc.*, **91**, 3976 (2008).
3. A.Ikesue, Y.L.Aung, *Nature Photonics*, **2**, 721 (2008).
4. O.L.Khasanov, Yu.L.Kopylov, V.B.Kravchenko et al., *Nanotechnics*, **2**, 3 (2008).
5. Yu.L.Kopylov, V.B.Kravchenko, S.N.Bagayev et al., *Opt. Mater.*, **31**, 707 (2009).
6. A.S.Kaygorodov, V.V.Ivanov, V.R.Khrustov et al., *J. Eur. Ceram. Soc.*, **27**, 1165 (2007).
7. W.-N.Wang, W.Widiyastuti, T.Ogi et al., *Chem. Mater.*, **19**, 1723 (2007).
8. S.Roy, W.Sigmund, F.Aldinger, *J. Mater. Res.*, **14**, 1524 (1999).
9. X.Zhang, H.Liu, W.He et al., *J. Alloys Comp.*, **372**, 300 (2004).
10. G.Yi, B.Sun, F.Yang, D.Chen et al., *Chem. Mater.*, **14**, 2910 (2002).
11. G.Liu, G.Hong, J.Wang et al., *J. Alloys Comp.*, **432**, 200 (2007).
12. V.V.Osipov, Yu.A.Kotov, M.G.Ivanov et al., *Laser Phys.*, **16**, 116 (2006).
13. S.N.Bagayev, V.V.Osipov, M.G.Ivanov et al., *Opt. Mater.*, **31**, 740 (2009).
14. J.-G.Li, X.Li, X.Sun et al., *Chem. Mater.*, **20**, 2274 (2008).
15. C.Greskovich, J.P.Chernoch, *J. Appl. Phys.*, **44**, 4599 (1973).
16. K.Takaichi, H.Yagi, J.Lu et al., *Appl. Phys. Lett.*, **84**, 317 (2004).
17. H.S.Yoo, H.S.Jang, W.B.Im et al., *J. Mater. Res.*, **22**, 2017 (2007).
18. J.Yang, Z.Quan, D.Kong et al., *Cryst. Growth & Design*, **7**, 730 (2007).
19. S.Sohn, Y.Kwon, Y.Kim, D.Kim, *Powder Technol.*, **142**, 136 (2004).
20. B.Aiken, W.P.Hsu, E.Matijevic, *J. Am. Ceram. Soc.*, **71**, 845 (1988).

Синтез монодисперсних кристалічних наносфер Y_2O_3 та $Y_2O_3:Nd^{3+}$ за методом гомогенного осадження

Ю.І.Пазюра, В.М.Баумер, О.М.Вовк, Т.Г.Дейнека, Р.П.Явецький

Методом гомогенного хімічного осадження з водних розчинів одержано монодисперсні кристалічні сфери Y_2O_3, $Y_2O_3:Nd^{3+}$ (1–10 ат. %) діаметром в інтервалі 100-260 нм з дисперсією за розміром ≤ 10 %. Вивчено процес формування наносфер кубічного оксиду ітрію при термічному розкладі аморфного прекурсору. Становлено вплив параметрів процесу осадження (концентрацій вихідних реагентів — іонів ітрію, неодиму, а також карбаміду) на розмір, форму, дисперсію та ступінь агломерації порошків.